Journal of Non-Crystalline Solids xxx (xxxx) xxx–xxx

Contents lists available at ScienceDirect

Journal of Non-Crystalline Solids

journal homepage: www.elsevier.com/locate/jnoncrysol

The influence of structure on the azo dye decolourization ability of ternary Fe-rich amorphous alloy

Peng Liu[a,b,*], Ji Liang Zhang[c], Li Zhong Zhao[d], Yi Fan Zhang[b], Chan Hung Shek[c,**]

[a] School of Environmental Science and Engineering, Tianjin University, Tianjin 300350, China
[b] Tianjin Capital Environmental Protection Group Co., Ltd, Tianjin 300381, China
[c] Department of Materials Science and Engineering, City University of Hong Kong, Kowloon Tong, Hong Kong, China
[d] School of Materials Science and Engineering, South China University of Technology, Guangzhou 510640, China

ARTICLE INFO

Keywords:
Structure
Constituent atoms
Zero-valent iron (ZVI)
jj coupling
Decolourization ability

ABSTRACT

$Fe_{66.3}B_{16.6}Y_{17.1}$ amorphous structures designed based on a competitive atomic cluster model shows excellent catalytic ability due to the competition between two different Fe-rich clusters $Fe_{11}Y_3$ and Fe_8B_2. In this work, it was demonstrated that the minor elements play a key role in the catalytic behaviors by changing the local structure around Fe. $Fe_{66.3}B_{16.6}Y_{17.1}$ based on $Fe_{11}Y_3$ and Fe_8B_2 clusters achieves the decolourization efficiency up to 99.2% on the azo dye Orange G (OG). The replacement of $Fe_{11}Y_3$ cluster by $Fe_{11}Zr_3$ or $Fe_{11}Nb_3$ leads to significantly deteriorated efficiencies of 13.2% for $Fe_{66.3}B_{16.6}Zr_{17.1}$ and 10.4% for $Fe_{66.3}B_{16.6}Nb_{17.1}$ at identical testing conditions. The analysis on their local structures and the bonding states of Fe revealed that the weak interactions between atoms in these structures are related to the decolourization ability and catalytic effect directly. X-ray photoelectron spectra show that the *jj* coupling in the Fe $2p^5 3d^7$ final state is a good predictor for the decolourization ability and catalytic effect of these Fe-rich amorphous structures.

1. Introduction

Iron is an inexpensive and eco-friendly material with mild reducing ability [1]. Iron powder was therefore usually used to reduce heavy metals [2], chlorinated organics [3,4], inorganic anions [5], dyes [6] and oxides [7] in sewage. Recently, we reported a new type of zero-valent iron (ZVI) existing in $Fe_{66.3}B_{16.6}Y_{17.1}$ amorphous structure with excellent decolourization ability at moderate conditions under which pure iron cannot achieve the same performance [8]. The $Fe_{66.3}B_{16.6}Y_{17.1}$ composition locates exactly at the intersection of two cluster composition lines, namely, Fe_8B_2-Y and $Fe_{11}Y_3$-B. For the Fe_8B_2 clusters, the B atoms occupy the interstice in a dense random packing of Fe atoms [9]. The $Fe_{11}Y_3$ cluster was extracted from the eutectic composition $Fe_{23}Y_6$ [10], which could be expressed as $[Fe_{22}Y_6]$-Fe_{glue}, where $Fe_{22}Y_6$ is a eutectic cluster and Fe_{glue} represents glue atom [11]. The amorphous alloy made by these two clusters has weakened bonds at the interstices or glue sites. With the weaker interactions between constituent atoms, the ZVI in $Fe_{66.3}B_{16.6}Y_{17.1}$ could be seen as 'pseudo iron' atoms frozen in the glassy state [8]. It has excellent capacity to decolorize azo dye and a catalytic effect was also generated spontaneously from the destabilized Fe-B-Y atomic arrangement [8].

In this investigation, we attempted to replace the expensive Y with less expensive elements. To avoid destabilizing the amorphous structure, Zr and Nb were selected to replace Y in the $Fe_{66.3}B_{16.6}Y_{17.1}$ structure based on considerations of atomic sizes and electronic configuration. The Zr and Nb have atomic sizes very close to that of Y, and the substitution is expected to induce minimal distortion of the $Fe_{66.3}B_{16.6}Y_{17.1}$ structure [12]. The similar electronic configuration of Zr and Nb to Y [13,14] also favors a structure similar to that of $Fe_{66.3}B_{16.6}Y_{17.1}$. The nominal composition of Fe-B-Zr/Nb was stipulated at $Fe_{66.3}B_{16.6}(Zr/Nb)_{17.1}$, to keep the atomic ratio identical to those of $Fe_{66.3}B_{16.6}Y_{17.1}$ [8]. For the preparation of $Fe_{66.3}B_{16.6}Y_{17.1}$, the compound Fe_8B_2 [9,15] was selected to mix with $Fe_{11}Y_3$ [10] to fabricate a ternary $Fe_{66.3}B_{16.1}Y_{17.1}$ structure (Fig. 1). The Zr or Nb was directly used to replace Y for preparing the $Fe_{66.3}B_{16.6}(Zr/Nb)_{17.1}$ amorphous alloys as illustrated in Fig. 1.

The $Fe_{66.3}B_{16.6}Zr_{17.1}$ and $Fe_{66.3}B_{16.6}Nb_{17.1}$ with amorphous structures were synthesized successfully using the same sample preparation technique for $Fe_{66.3}B_{16.6}Y_{17.1}$ [8]. As expected, $Fe_{66.3}B_{16.6}Zr_{17.1}$ and $Fe_{66.3}B_{16.6}Nb_{17.1}$ show similar amorphous structure and decolourization ability to each other. However, their structure is quite different from that of $Fe_{66.3}B_{16.6}Y_{17.1}$ and their decolourization abilities are significantly weaker compared with $Fe_{66.3}B_{16.6}Y_{17.1}$. The side by side comparisons of atomic structures, electronic structures and

* Correspondence to: P. Liu, School of Environmental Science and Engineering, Tianjin University, Tianjin 300350, China.
** Corresponding author.
E-mail addresses: 158605123@qq.com (P. Liu), apchshek@cityu.edu.hk (C.H. Shek).

http://dx.doi.org/10.1016/j.jnoncrysol.2017.10.038
Received 18 August 2017; Received in revised form 17 October 2017; Accepted 18 October 2017

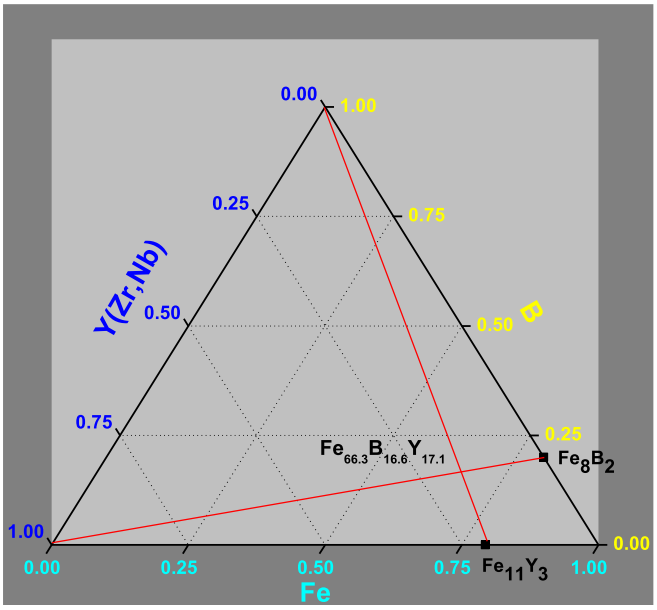

Fig. 1. Ternary phase diagram of $Fe_{66.3}B_{16.6}Y_{17.1}$ and Y was replace by Zr and Nb.

decolourization of the three alloys reveal the correlations among structural design, bonding states of Fe and decolourization activities unambiguously. We also found that the *jj* coupling in the Fe $2p^5 3d^7$ final state is a telltale parameter to indicate the decolourization ability and catalytic effect of ternary Fe-rich amorphous structures.

2. Experimental

The raw materials were commercially available with purity higher than 99.9% and were melted at least three times to improve homogeneity before use. The master ingot of $Fe_{66.3}B_{16.6} \times {}_{17.1}$(X = Y, Zr, Nb) were fabricated by arc-melting the X and Fe-B alloy in high-vacuum (0.002 Pa) under Ti-gettered Argon atmosphere. The amorphous structure $Fe_{78}B_{14}Si_8$ [16] was selected for a comparison of structure and decolourization ability. The foils were produced from the ingots by a single roller melt-spinning apparatus and were cut to approx. 2 mm × 15 mm pieces before use. Pure iron powder and analytical grade Orange G ($C_{16}H_{10}N_2Na_2O_7S_2$, MW = 452.37 g/mol) were purchased from ALDRICH and used directly.

The decolourization tests were undertaken at room temperature (20 ± 2 °C). The dosage was set at a ratio 0.067 g/5 mL (foil/OG). The OG aqueous solution has concentration of 100 mg/L and pH = 6.5. The mixture was held in sealed glass bottle under continuous stirring. About 1.0 mL filtrate was taken out at 30 min intervals and diluted 4.5times for subsequent UV–Vis spectrum measurement.

The amorphous structure of as-cast foils was confirmed by X-ray Diffraction (XRD, Philips X'pert X-ray diffractometer) with Cu-Kα radiation (0.15406 nm). The full width at half maxima (FWHM) of amorphous hump is much larger than the width induced by the instrument (no > 0.07°). The uncertainties of determined FWHM and peak position are generally < 0.01°, and thus not listed. The phase identification of annealed samples was conducted by Bruker D8 Advance with Mo-Kα radiation (λ = 0.7097 Å). X-ray photoelectron spectroscopy (XPS, ULVAC-PHI 5802 system) with mono chromatized Al K_α radiation (1486.6 eV) was employed to characterize the valence band (VB) and core level structure of the Fe in the samples. The Fe 2p spectra were fitted by Lorentzian-Gaussian method. The fitted curve had maximal overlap area. UV–Vis spectrometer (Perkin Elmer, Lambade2S) was used to collect absorption spectrum of the filtrates. Inductively Coupled Plasma Optical Emission Spectrometry (ICP-OES, PerkinElmer Optima™ 2100 DV) was employed to identify the elements leached out into the OG solution. Each sample was measured three times in the experiment. The mean value with standard deviation (SD) was recorded and presented in supporting materials. Scanning Electron Microscope (SEM with EDX, JEOL JSM 820, JEOL Ltd. and Oxford Instruments INCA X-Sight 7109.) was used for examining the surface morphologies of the foils after immersion in OG solution. X-Ray Micro fluorescence spectrometer (XRMF, EDAX Eagle III) with 40 W X-Ray tube (Mo) and 1 mm spot aperture was used to verify the content of metals. In the measurement, several locations on the ribbon surface were selected to check the atomic ratio. The mean value with SD was exhibited in supporting materials.

3. Results

3.1. Characterization of samples

As shown in Fig. 2, the halo in XRD patterns confirmed the amorphous nature of these samples. Despite their amorphous nature, the positions and full widths at half maximum (FWHW) of these halo peaks vary clearly among these samples (Table1). The typical peak position of

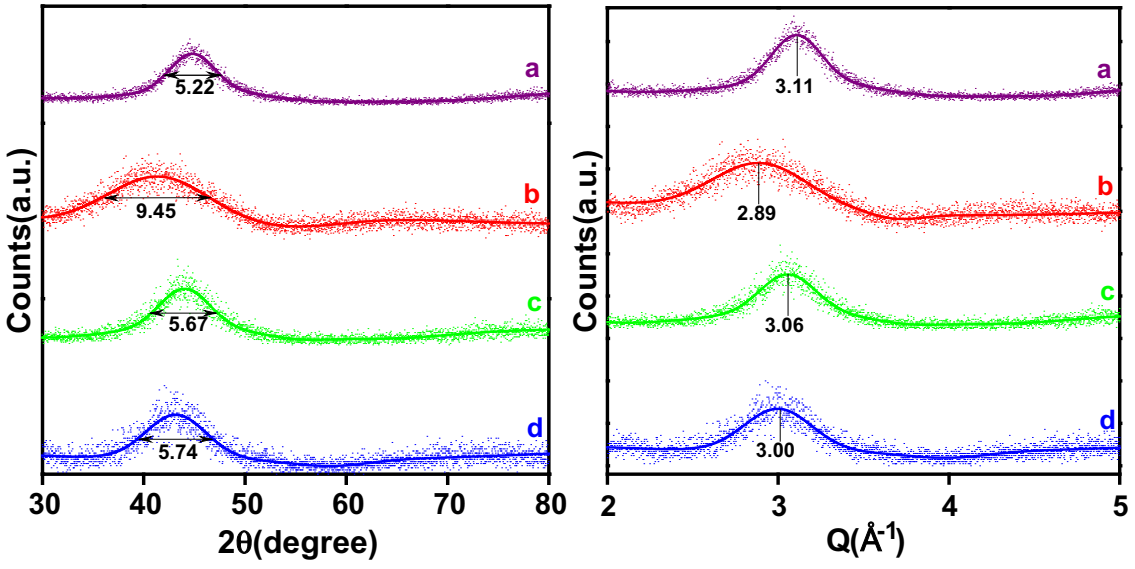

Fig. 2. The XRD patterns of (a) $Fe_{78}B_{14}Si_8$, (b) $Fe_{66.3}B_{16.6}Y_{17.1}$, (c) $Fe_{66.3}B_{16.6}Nb_{17.1}$ and (d) $Fe_{66.3}B_{16.6}Zr_{17.1}$.